

Dosimetric investigation of high dose rate Ir-192 source with Monte Carlo method

H. Acun^{1*}, A. Bozkurt², G. Kemikler³

¹Harran University, Faculty of Medicine, Department of Biophysics, Osmanbey Campus, 63300 Sanliurfa, Turkey

²Akdeniz University, Faculty of Engineering, Department of Biomedical Engineering, Antalya, Turkey

³Istanbul University, Institute of Oncology, Department of Medical Physics, 34390 Capa, Istanbul, Turkey

ABSTRACT

► Original article

*Corresponding authors:

Dr. Hediye Acun,

Fax: +90 414 3183192

E-mail:

acunhediye@yahoo.com

Revised: April. 2016

Accepted: Oct. 2016

Int. J. Radiat. Res., July 2017;
15(3): 241-249

DOI: 10.18869/acadpub.ijrr.15.3.241

Background: This study aims to calculate the air-kerma strength (S_K), the dose rate constant (Λ) and the dose rate profiles of a Gammamed 12i Ir-192 source by using the Monte Carlo technique and to compare the dose rate values with those calculated by the Abacus HDR treatment planning system (TPS).

Materials and Methods: Air-kerma strength (in units of U; 1 U = $\mu\text{Gy m}^2 \text{ h}^{-1}$) and the dose rate constant (Λ) of a Gammamed 12i Ir-192 source were computed with the Monte Carlo-based code MCNP. For a single dwell position, profiles of dose rate per air kerma rate strength (in unit of U) along the x axis were obtained with MCNP and compared with data from the Abacus TPS at $y=0, 1$, and 2 cm. **Results:** The air-kerma strength and the dose rate constant of the source were calculated to 9.98×10^{-8} U and $1.106 \text{ cGy h}^{-1} \text{ U}^{-1}$, respectively. The maximum dose differences between MCNP and TPS along the x axis were found to be 1.3, 3.7 and 5.4% at distances more than 1 cm away from the source center for $y=0, 1$ and 2 cm planes, respectively.

Conclusion: The dose rate profiles calculated with MCNP and by the TPS show good agreement except for points located beyond the tip of the source.

Keywords: Monte Carlo, high dose rate brachytherapy, Ir-192.

INTRODUCTION

In high dose rate (HDR) brachytherapy, the prescribed treatment dose of irradiation is given to the patient in a few fractions, in high dose rates (dose rate $> 2 \text{ Gy/min}$) and in short time sequences ⁽¹⁾. In this treatment modality, the dose distribution around the applicator is obtained from commercial treatment planning systems (TPS) which use various optimization methods to obtain the most appropriate irradiation scenario ⁽²⁾. Previously dose rates for HDR treatment planning systems were calculated by using conventional calculations based on isotropic point source approximation. In recent years, however, many TPS algorithms base their calculations on the TG-43 formalism ⁽³⁾.

In classical dose calculation with point source approximation, the dose rate at a point of interest depends on the activity of the source.

The exposure rate is thus measured per activity in air, where the Meisberger polynomial describes the absorption and scatter effects of the media ⁽³⁾. The TG-43 formalism, on the other hand, is based on the dosimetry parameters used for absolute dose calculation around the source, i.e. the air-kerma strength (S_K), the dose rate constant (Λ), the geometry factor $G(r, \theta)$, the radial dose function $g(r)$ and the 2D (two dimensional) anisotropy factor. These parameters are either measured with suitable detectors or calculated with Monte Carlo simulation techniques ⁽⁴⁾. Neither classical nor TG-43 dose calculation methods take the geometry and the material composition of the source into account. In addition, the TG-43 formalism has the advantage of using absolute dose calculations based on the dosimetry parameters as they are defined in water.

Verification of dose distribution in HDR

brachytherapy is quite challenging due to the possible presence of high-dose regions close to the source as well as the rapidly decreasing character of the dose at farther distances ⁽⁵⁾. Therefore dosimetric verification of HDR sources should be carried out either through measurements or by calculations. However, the type of dosimeter used for measurements is important due to the high signal-to-noise ratio that can occur at farther distances. Other challenges with detectors are positioning difficulties in areas closely around the source ⁽⁵⁾. Since the source geometry and the irradiation parameters can be more realistically modeled with Monte Carlo simulations, it becomes a more reliable and useful method for validation of TPS dose distributions ⁽⁶⁾. In addition to this, Monte Carlo simulations have often been used to calculate TG-43 dosimetry parameters ^(7,8).

In recent years, several studies have used Monte Carlo simulations for verification of TPS dose distributions around various types of sources and applicators. Anagnostopoulos *et al.* generated an esophagus irradiation including 13 source positions with the Plato TPS (BPS version 14.2.4) based on the TG-43 formalism ⁽⁹⁾. The same irradiation parameters were modeled with MCNPX Monte Carlo code in a human equivalent mathematical phantom and the results were compared with those calculated by the TPS. While good correspondence were reported between TPS and MC calculated target volume doses, differences were observed for doses of surrounding organs in risk volumes. Lypertpoulo *et al.* used MCNPX code to simulate a cylindrical applicator in shielded and unshielded irradiation scenarios and compared dose distributions around it with those calculated by the Plato TPS (BPS, v. 14.2.7) ⁽¹⁰⁾. In another study, dose distribution obtained with the Plato HDR TPS (based on the TG-43 formalism) and MCNP around a MicroSelectron HDR Ir-192 source was studied by Mowlavi *et al.* ⁽¹¹⁾. They measured the dose profile along the y and x axis with Gafchromic RTQA films and compared the results with those calculated with MCNP. Differences between dose profiles from MC and film were observed with increasing distance from the source center, due to uncertainty of the

positioning of the film during the measurements.

The aim of this study was to verify the x-dose rate profiles per air-kerma strength calculated by the Abacus TPS around single and multiple dwell positions of a GammaMed HDR 12i Ir-192 (Varian Oncology Systems, Palo Alto, USA) source with the Monte Carlo radiation transport code MCNP. In order to do so the TG-43 dosimetry parameters, namely the air-kerma strength (S_K) and the dose rate constant (Λ) of the source, were calculated with MCNP.

MATERIALS AND METHODS

The Abacus TPS (Isotopen-technik Dr. Sauerwein GMBH, Haan, West Germany) uses a classical dose calculation method based on point source approximation (Sievert integral and the Meisberger polynomial). The dose rate is calculated by multiplying the Meisberger polynomial with source activity, exposure rate per activity measured in air and anisotropy factor as a function of distance and angle (r, θ) between the source and the point of interest. The Meisberger polynomial includes the effects of absorption and scattering caused by photons at certain distances. Different irradiation settings can be created by varying the number of dwell positions, the irradiation time for each dwell position and the distance between two dwell positions for each applicator.

Dose profiles around the Gammamed 12i Ir-192 source (Varian Oncology Systems, Palo Alto, USA) (single dwell position), with an activity of 10 Ci, were obtained with the Abacus TPS. The source was assumed to lie along the y axis and the dose profiles were obtained along the x axis (perpendicular to the source) in planes at $y=0, 1$ and 2 cm. As a clinical example, an irradiation scenario for a 2 cm long source was created in the TPS with 5 dwell positions, all with different irradiation times (the distances between the dwell positions were 0.5 cm). The dose profiles along the x axis at $y=0$ cm (source on-axis) were obtained for comparison purposes. The doses calculated by TPS were absolute doses in Gy. To convert the data into the format

dose rate per U, the absolute doses were divided by irradiation time and the air-kerma strength (in units of U; $1U = \mu\text{Gy m}^2 \text{ h}^{-1}$) of the source. The latter was obtained from the source certificate. The findings were then compared with those from the MCNP code.

Monte Carlo N-Particle (MCNP) Transport Code

In recent years the Monte Carlo method has become rather frequently used for computations involving radiation transport problems ⁽¹²⁾. MCNP is one of the widely used Monte Carlo-based codes in both clinical and industrial settings ⁽¹³⁾. In this study the irradiation geometries and the properties of the materials involved were first modeled with MCNP in order to calculate the dosimetry parameters and the dose profiles. The MCNP code, which was developed in Los Alamos National Laboratory (LANL), can calculate the transport and interactions of various particles for an extensive range of energies in arbitrary 3-D geometries.

The source examined in this study was an encapsulated GammaMed 12i Ir-192 source contained in the after-loading device for HDR applications. The source was composed of a central cylindrical core made of iridium (density: 22.42 g/cc; diameter: 0.6 mm; height: 3.5 mm) and a surrounding outer steel capsule (outer diameter: 1.1 mm; thickness: 0.1 mm) and cable (outer diameter: 1.1 mm), both made of stainless steel (density: 7.92 g/cc; weight fraction: 19 % Cr, 20 % Mn, 69.5 % Fe, 9.5 % Ni). All geometries and material compounds of the source were modeled with MCNP as shown in figure 1. The source and detectors were located in a water phantom with a volume of $30 \times 30 \times 30$ cc.

Calculated dose values of brachytherapy sources are generally normalized to the air-kerma strength (S_K) in units of U ($1U = \mu\text{Gy m}^2 \text{ h}^{-1}$) in the literature (14, 15). This TG-43 dosimetry parameter is specific to the radionuclide content of the source and its value may vary depending on the details of the source geometry. Hence S_K should be computed for each of the modeled sources. For air-kerma strength calculation, 36 spherical detectors were positioned at equal angle intervals (10 degrees)

in a circle with 1 m radius around the source (standing in vertical position). The detectors were all modeled with real geometries and material compounds. Calculations were done in vacuum as recommended by the TG-43 report. The dose rate constant (Λ) is the ratio of the dose rate $D(r_0, \theta_0)$ at the reference point (1 cm from the source) in relation to the air-kerma strength (S_K). The average value from the readings of four detectors (positioned 1cm from the source, with 90 degree angle intervals) was calculated in order to compute the dose rate, $D(r_0, q_0)$. The dose rate constant (Λ) was then obtained as the ratio of the dose rate relative to the air-kerma strength.

Spherical dose cells (with 0.25 cm radius) were positioned along the source (y axis) at $z = 1, 2$ and 5 cm planes (for literature comparison) and along the x axis at $y = 0, 1$ and 2 cm planes (for TPS validation). As a clinical example, an irradiation geometry with a length of 2 cm was obtained with TPS by formation of a source train. For multiple sources of 2 cm length, the dose detectors cells were located along +x axis at the center of the source train ($y = 0$ cm). An air sphere (density: 0.001205 g/cc; weight fraction: 0.0124% C, 75.5268% N, 23.1781% O, 1.2827% Ar; radius of 100 cm) was modeled around the water phantom and the outside of it was defined to have zero importance. The irradiation geometries created with MCNP are shown in figure 2.

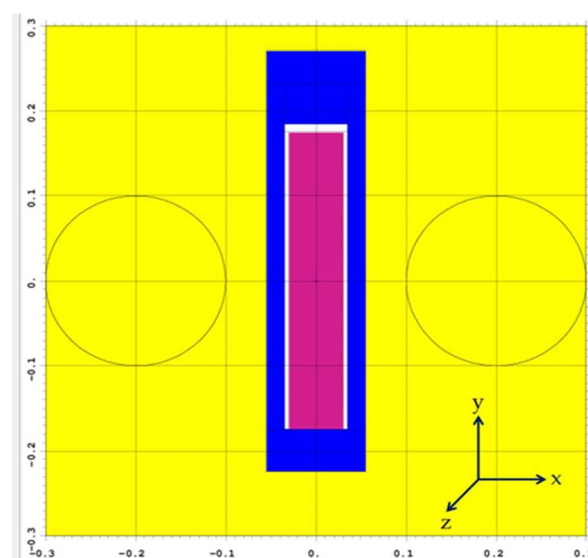


Figure 1. The GammaMed 12i Ir-192 source geometry plotted with MCNP. All dimensions are in units of cm.

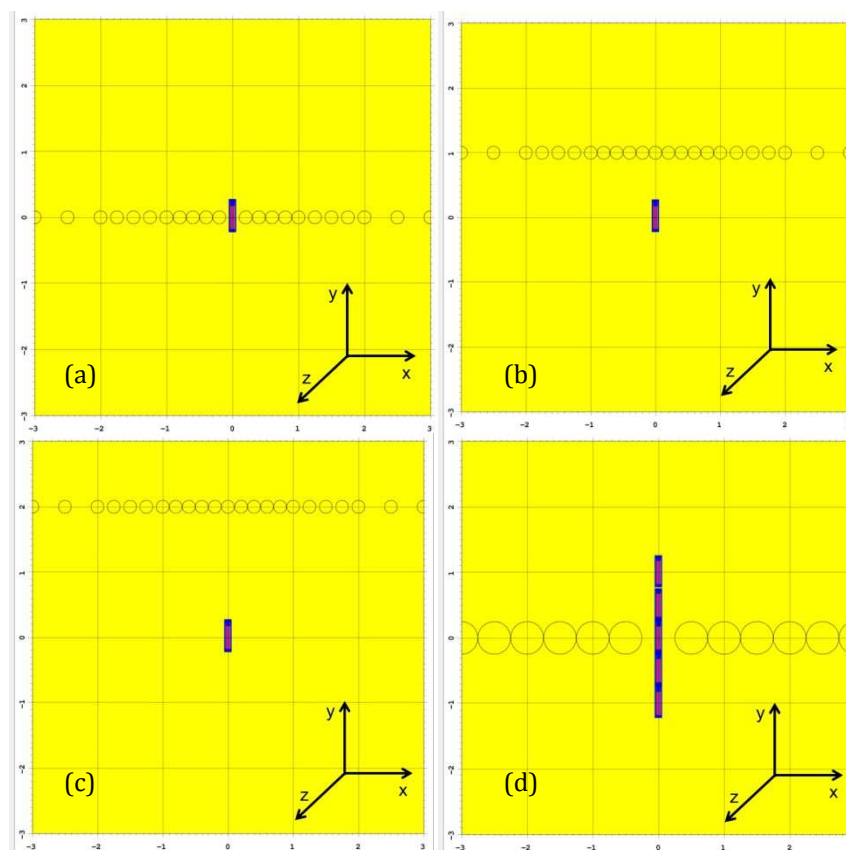


Figure 2. The coronal view of the source and the detectors obtained from a MCNP plot. All dimensions are in units of cm. a) detectors are at $y=0$ cm, b) detectors are at $y=1$ cm, c) detectors are at $y=2$ cm d) detectors are at $y=0$ cm for multiple sources, 2 cm in length.

In the simulations, only photon interactions were taken into account, without contributions from secondary particles. Flight directions of the source particles were not specified (4π isotropic distribution). The energy spectrum of the Ir-192 source was determined so as to include both the gamma and the X-ray lines of the isotope. As a result the photon energy spectrum of the source included 33 energies (in the range of 61.49 keV and 1378.3 keV; the most probable energy is 316.51 keV with an intensity of 82.86%) with 2.243 photons per disintegration⁽¹⁶⁾.

The absolute dose recorded by the detectors was defined via the energy deposition (in units of MeV g^{-1} per particle) tally (F6) of MCNP. The simulations were run for 100 million photon entries to ensure statistical errors less than 2%.

The absolute dose in units of U ($\mu\text{Gy m}^2 \text{h}^{-1}$) per activity was obtained by applying the following mathematical expression to the

detector readings (in unit of MeV/g).

$$(\text{MeV/g/particle}) \times (1.602 \times 10^{-13} \text{ J/MeV}) \times (10^3 \text{ g/kg}) \times (10^6 \text{ mGy/Gy}) \times (2.243 \text{ particle/disintegration}) \times (3600 \text{ s/h})$$

RESULTS

The average air-kerma strength (S_K) for the MCNP model was calculated to 9.98×10^{-8} U (min: 9.444×10^{-8} ; max: 1.03×10^{-7}). The distribution of S_K values obtained by the MCNP detectors in air as a function of θ (the angle between source and detector centers) is presented in figure 3. The air-kerma strength per activity reported in the Gammamed 12i Ir-192 source certificate was $1.10 \times 10^{-7} \mu\text{Gy m}^2 \text{h}^{-1} \text{Bq}^{-1}$.

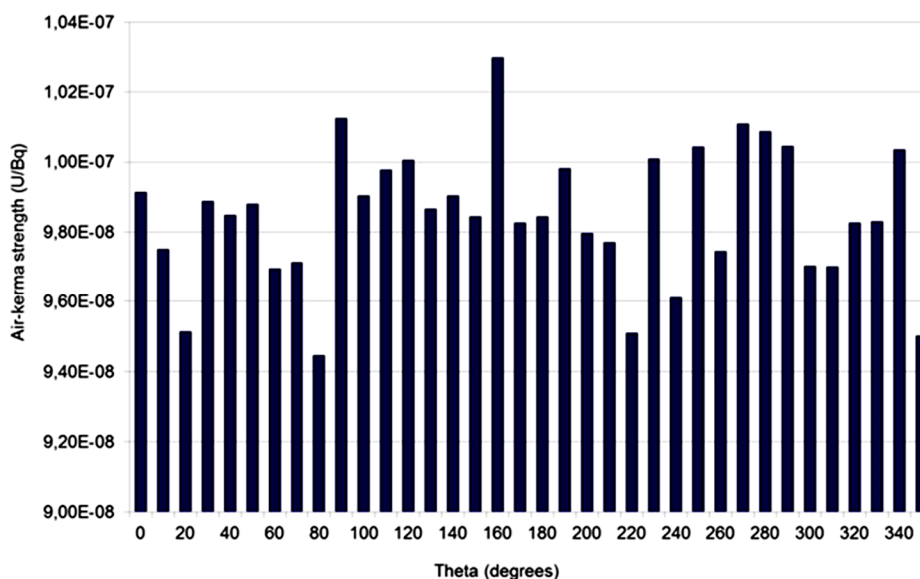


Figure 3. Variation of air kerma rate strength as a function of angle (Theta, θ) between the detector and the source center.

The dose rate value in the reference point D (r_0, θ_0) was computed to be 1.106×10^{-7} cGy h⁻¹ per activity. The dose rate constant (Λ) was calculated to 1.106 cGy h⁻¹ U⁻¹ by dividing the dose rate value D (r_0, θ_0) with the air-kerma strength (S_K) of the Gammamed 12i Ir-192 source.

Since the dose values obtained from the Abacus treatment planning system were in units of Gy, the dose rate values per air-kerma strength (cGy/h/U) were calculated by taking into account the source irradiation time and SK values.

Table 1 contains a comparison between the dose rates per U calculated with MCNP and those of Ballester *et al.* ⁽¹⁵⁾, for three different planes ($z = 1, 2$ and 5 cm) along the source (y axis). For those different planes the differences between MCNP and Ballester's results were found to be less than 3% in the interval between -5 and 5 cm. The dose rate difference was found to be less than 1% at close distances, less than 1 cm from the source center. The largest difference was found to be 3.85% for all three planes, for farther distances ($y > \pm 6$ cm) from the source center.

The dose rate graphs per air-kerma strength along the x axis for a single Ir-192 source, calculated by Abacus TPS and with MCNP, are

shown in figure 4a, b, c, for $y = 0, 1, 2$ cm planes, respectively. Dose rates per U calculated by the TPS were found to be 19.4 % and 20.5% higher than those obtained with MCNP at close distances ($x=0.2$ mm) from the source tip, for $y = 1$ and 2 cm axes. The biggest differences between MCNP and TPS were observed for points close to the source, since electron transport is not taken into account in MCNP simulations. The maximum differences between MCNP and TPS were 3.4 %, 4.9 % and 12.8 % for $y = 0, 1$ and 2 cm planes respectively, at distances farther than 4 mm away from the source center ($x > 4$ mm). For distances farther away than 1 cm from the source center ($x > 1$ cm), the largest dose rate differences between the two calculation techniques were 1.0%, 3.7% and 5.4% for $y = 0, 1$ and 2 cm planes, respectively.

Figure 4d shows a graph of dose rates (in unit of cGy/h/U) calculated with MCNP and by TPS along the x axis at the center plane of the multiple sources ($y = 0$ cm) for the 2 cm long irradiation geometry. The difference between MCNP and TPS decreases up to a distance of 4 cm from the source center, and thereafter increases. The maximum dose rate difference was computed to 4.6% at close distances (less than 1 cm) from the multiple source center.

Table 1. Dose rate per U (unit of air kerma strength) calculated with MCNP and obtained from Ballester et al. (15) along the source (y axis) for z= 1, 2 and 5 cm planes.

	z = 1 cm			z = 2 cm			z = 5 cm		
y (cm)	MCNP cGy/h/U	Ballester cGy/h/U	diff. (%)	MCNP cGy/h/U	Ballester cGy/h/U	diff. (%)	MCNP cGy/h/U	Ballester cGy/h/U	diff. (%)
8-	0.01232	0.01280	3.85-	0.01317	0.01340	1.75-	0.01079	0.01120	3.84-
6-	0.02302	0.02330	1.23-	0.02317	0.02390	3.14-	0.01662	0.01720	3.51-
5-	0.03380	0.03380	0.01-	0.03325	0.03390	1.96-	0.02131	0.02130	0.06
4-	0.05336	0.05350	0.27-	0.04993	0.05070	1.55-	0.02646	0.02650	0.17-
3.5-	0.06983	0.07020	0.54-	0.06350	0.06350	0.00	0.02889	0.02940	1.76-
3-	0.09595	0.09500	0.99	0.08138	0.08110	0.34	0.03195	0.03250	1.71-
2.5-	0.13722	0.13500	1.62	0.10492	0.10500	0.08-	0.03561	0.03560	0.04
2-	0.20143	0.20300	0.78-	0.13757	0.13700	0.41	0.03836	0.03850	0.36-
1.75-	0.25475	0.25400	0.30	0.15544	0.15600	0.36-	0.03940	0.03980	1.02-
1.5-	0.32175	0.32400	0.70-	0.17837	0.17700	0.77	0.04118	0.04120	0.04-
1.25-	0.41767	0.41900	0.32-	0.19973	0.20100	0.64-	0.04179	0.04230	1.22-
1-	0.54716	0.54600	0.21	0.22571	0.22400	0.76	0.04287	0.04330	0.99-
0.8-	0.67426	0.67300	0.19	0.24196	0.24300	0.43-	0.04353	0.04390	0.84-
0.6-	0.81438	0.81800	0.44-	0.25788	0.25900	0.43-	0.04441	0.04440	0.02
0.4-	0.96345	0.96200	0.15	0.27100	0.27200	0.37-	0.04544	0.04480	1.42
0.2-	1.07503	1.07000	0.47	0.27756	0.28000	0.88-	0.04521	0.04510	0.25
0	1.12207	1.11800	0.36	0.28248	0.28300	0.18-	0.04515	0.04510	0.11
0.2	1.07061	1.07000	0.06	0.28065	0.28000	0.23	0.04413	0.04510	2.21-
0.4	0.95794	0.96300	0.53-	0.26890	0.27200	1.15-	0.04481	0.04490	0.19-
0.6	0.81479	0.81800	0.39-	0.25725	0.25900	0.68-	0.04430	0.04450	0.44-
0.8	0.67175	0.67300	0.19-	0.24082	0.24300	0.90-	0.04387	0.04400	0.29-
1	0.54790	0.54700	0.16	0.22299	0.22500	0.90-	0.04364	0.04330	0.77
1.25	0.41863	0.42000	0.33-	0.20073	0.20100	0.13-	0.04186	0.04240	1.28-
1.5	0.32397	0.32500	0.32-	0.17569	0.17800	1.31-	0.04109	0.04120	0.28-
1.75	0.25426	0.25500	0.29-	0.15618	0.15600	0.12	0.03923	0.04000	1.96-
2	0.20304	0.20400	0.47-	0.13704	0.13700	0.03	0.03796	0.03860	1.68-
2.5	0.13591	0.13600	0.07-	0.10487	0.10500	0.12-	0.03602	0.03560	1.18
3	0.09418	0.09640	2.36-	0.08082	0.08150	0.84-	0.03187	0.03260	2.30-
3.5	0.07108	0.07130	0.31-	0.06335	0.06410	1.18-	0.02874	0.02950	2.65-
4	0.05352	0.05470	2.21-	0.05112	0.05120	0.15-	0.02660	0.02670	0.36-
5	0.03524	0.03490	0.97	0.03378	0.03430	1.53-	0.02105	0.02140	1.68-
6	0.02364	0.02420	2.37-	0.02373	0.02430	2.41-	0.01721	0.01720	0.09
8	0.01299	0.01340	3.19-	0.01327	0.01370	3.24-	0.01097	0.01130	2.96-

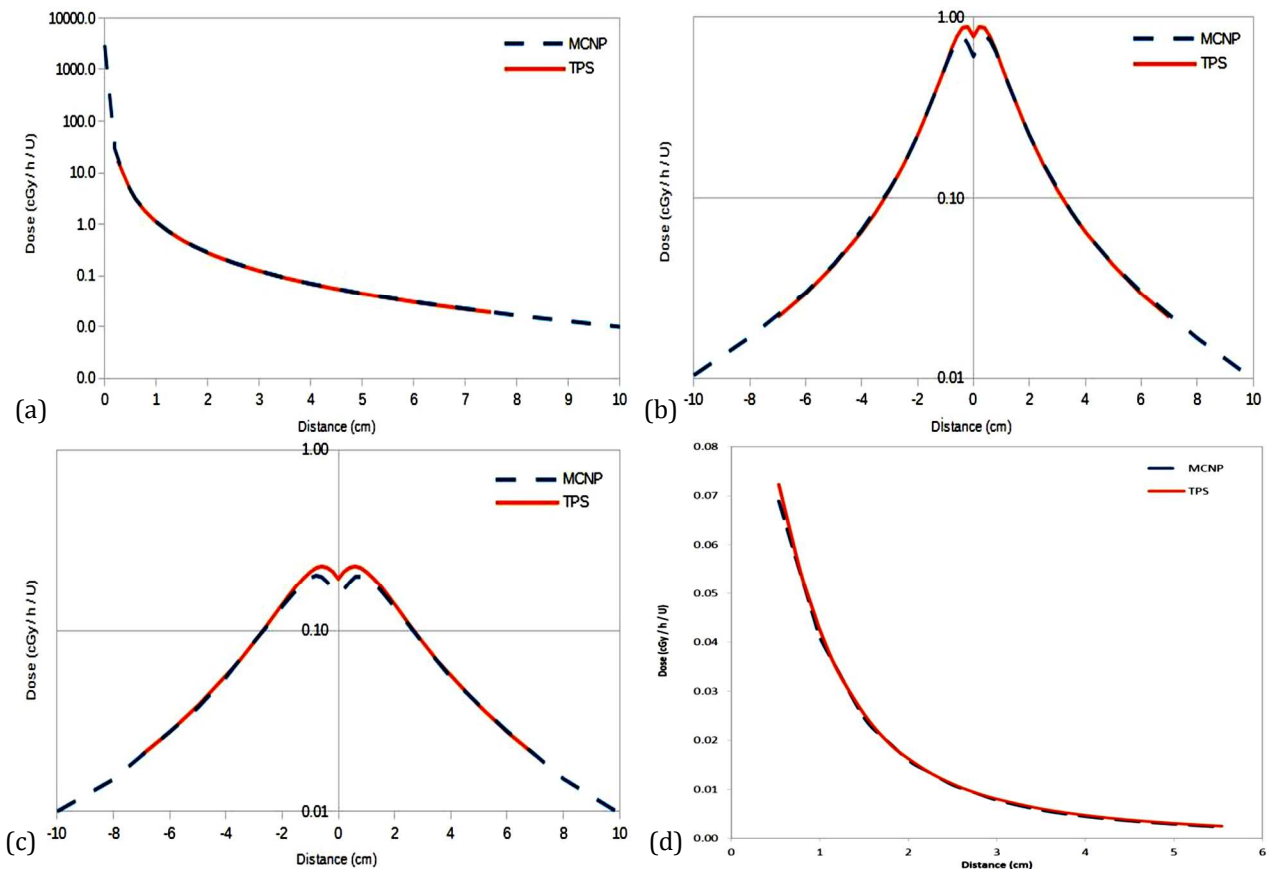


Figure 4. Dose rate per U (air kerma unit) obtained by TPS and MCNP as a function of distance. a) for single source along +x axis at $y=0$ cm plane, b) for single source along x axis at $y=1$ cm plane, c) for single source along x axis at $y=2$ cm plane, d) for multiple sources, 2 cm in length along +x axis at $y=0$ cm plane.

DISCUSSION

In treatments with high dose gradients such as HDR, the accuracy of the delivered dose is very important. The Monte Carlo technique can provide calculations of radiation interactions in various media and is quite often used to estimate dosimetry parameters and verify dose distributions of brachytherapy sources. In this study, MCNP was used to calculate the dose rate profiles per air-kerma strength of a Gammamed 12i Ir-192 source in different planes along y and x axes. The results were compared with the Abacus TPS and literature findings.

In previous studies, several Monte Carlo codes have been used in order to calculate TG-43 dosimetry parameters of different HDR brachytherapy sources. Gammamed HDR 12i and Plus Ir-192 sources were modeled with Geant3 MC Code by Ballester *et al.* (15). They

found the dose rate constant to be $1.118 \text{ cGy h}^{-1} \text{ U}^{-1}$ for both sources. Taylor *et al.* calculated the dose rate constant to $1.117 \text{ cGy h}^{-1} \text{ U}^{-1}$ for a Gammamed 12i Ir-192 source by using EGSnrc (17). In our study, the dose rate constant of a Gammamed 12i Ir-192 source was, by using MCNP, computed to $1.106 \text{ cGy h}^{-1} \text{ U}^{-1}$. Our result is in good agreement with those two in the literature as it differs no more than 1 % from them although a different MC code was used for the same source. Lopez *et al.* calculated the air-kerma strength to $9.87 \times 10^{-8} \text{ U Bq}^{-1}$ for a Gammamed plus Ir-192 source (18). We calculated the air-kerma strength for a Gammamed 12i Ir-192 source and found the constant to be $9.998 \times 10^{-8} \text{ U Bq}^{-1}$. Our dosimetry parameters have consistency with literature findings.

There is good consistency between comparisons of our study (MCNP) and Ballester's findings for dose rate per air-kerma strength

along the source axis (y axis) in three different planes ($z=1, 2$ and 5 cm). The difference is less than 3% at close distances from the source (up to 5 cm from the source center) for all planes. Larger differences, up to 3.85 %, were observed at extremity points ($y > \pm 6$ cm). This could be attributed to the fact that we used MCNP code in our study whereas GEANT3 MC code was used in Ballaster's study.

There are several studies related to verification of HDR treatment planning systems in the literature. Shwetha *et al.* ⁽²⁾ compared dose distribution around a single dwell position. Distributions for an Ir-192 source were calculated with Abacus (which uses classical calculation based on point source approximation) and BrachyVision (based on TG-43 formalism) treatment planning systems. The largest differences between the two treatment planning systems were observed along the source axis ($\theta=0$). The mean dose difference between the treatment planning systems was found to be 3.78 % towards the distal end of the cable while it was 19.82 % at the proximal end. The reason for this significant difference was thought to be different anisotropy factors of the two treatment planning systems, which use different calculation methods. Further, small dose differences, up to 1.88%, were observed along the perpendicular axis of the source. Both treatment planning systems (classical calculation and TG-43 formalism based) were in good consistency except from at the proximal end of the cable ⁽²⁾. The absorbed dose $D(r, \theta)$ strongly depends on the radial distance r and the angle between the source center and the point of interest. We also observed larger discrepancies between TPS and MCNP at the points (lying along source axis) which have large theta (θ) angles between the source center and the interested point. This discrepancy between TPS and MC along the source axis may have been caused by the anisotropy factor which is used in the algorithm of the TPS whereas MCNP calculates doses by taking into account radiation interactions.

Naseri et al. compared the dose distributions calculated with MCNP and the GZP6 treatment planning system around a HDR Co-60 braid type

source ⁽¹⁹⁾. A difference of about 15% was found between the two methods at close distances from the source, because of high dose gradient. Dose differences were calculated to be less than 2 % at distances farther than 7 mm away from the source. The authors reported differences up to 25% beyond the applicator tip, caused by the attenuation of steel balls located in the encapsulated source seed which is not implemented in the algorithm of the TPS. In our study, we also found the largest differences, up to 20.5 %, at the points away from the source tip. The Gammamed 12i source has an outer steel capsulation with a thickness of 0.1 mm and this amount is 0.86 mm at the tip of it. Because of this steel absorption, which is not taken into account by the algorithm of the TPS, we found deviations between MCNP and TPS results since the source was modeled realistically with MCNP.

Wallace *et al.* studied the transverse radial dose distribution around the Nucletron MicroSelectron Ir-192 source with MCNP. They found significant differences between the results of MCNP and the treatment planning system in the near field (radius less than 1 cm). This deviation was attributed to the treatment planning system, which uses an algorithm based on point source with attenuation and scatter corrections based on the Van Kleffen and Starr or Meisberger equations ⁽²⁰⁾. Similarly, we found bigger differences between MCNP and TPS at the points close to the source. Our TPS also has a classical dose calculation algorithm which uses the Meisberger polynomial to take account of the effects of absorption and scattering. It could be said that the other reason for these bigger differences is that the electron transport was not taken into account in the MCNP simulations.

CONCLUSION

In this study absolute dose rate per air-kerma strength values around the Ir-192 source were calculated with MCNP and the Abacus TPS in three different y planes along the x axis. Larger dose rate differences between MCNP and TPS were observed beyond the tip of

the source due to the steel capsulation of the source and large theta (θ) angle between the source and the interested point. Apart from points located beyond the source ($q@ 90$), TPS and MCNP dose rate profiles per air kerma strength are consistent with each other. As a conclusion, MCNP can be used for calculation of dosimetry parameters of HDR sources and for verification of the dose rates calculated by HDR treatment planning systems.

Conflicts of interest: Declared none.

REFERENCES

1. Khan FM and Gibbons JP (2003) High Dose Rate Brachytherapy. In: The Physics of Radiation Therapy. 3th. ed. Lippincott: Williams & Wilkins; Baltimore, Maryland. USA.
2. Shwetha B, Ravikumar M, Supe SS, Sathiyar S, Lokesh V, Keshava SL (2012) Dosimetric evaluation of two treatment planning system for high dose rate brachytherapy applications. *Med Dosim*, **37**: 71-75.
3. Rivard MJ, Venselaar JLM, Beaulieu L (2009) The evolution of brachytherapy treatment planning. *Med Phys*, **36**: 2136-2153.
4. Rivard MJ, Coursey BM, DeWerd, LA et al (2004) Update of AAPM Task Group No. 43 Report: A revised AAPM protocol for brachytherapy dose calculations. *Med Phys*, **31**: 633-674.
5. Perez-Calatayud J, Cabanero DG, Ballester FB (2009) Monte Carlo application in brachytherapy dosimetry. In: Lemaigne Y, Caner A (Eds.), radiotherapy and brachytherapy. Springer Netherlands, p. 239-240.
6. Mesbahi A (2008) Radial dose functions of GZP6 intracavitary brachytherapy ^{60}Co sources: treatment planning system versus Monte Carlo calculations. *Iran J Radiat Res*, **5**:181-186.
7. Bidmeshki NB, Sohrabpour M, Mahdavi SR (2014) Dosimetric characterization of a high dose rate ^{192}Ir source for brachytherapy application using Monte Carlo simulation and benchmarking with thermoluminescent dosimetry. *Int J Radiat Res*, **12**: 265-270.
8. Granero D, Vijande J, Ballester F, Rivard MJ (2011) Dosimetry revisited for the HDR ^{192}Ir brachytherapy source model mHDR-v2. *Med Phys*, **38**: 487-494.
9. Anagnostopoulos G, Baltas D, Pantelis E, Papagiannis P, Sakelliou L (2004) The effect of patient inhomogeneities in oesophageal ^{192}Ir HDR brachytherapy: a Monte Carlo and analytical dosimetry study. *Phys Med Biol*, **49**: 2675-2685.
10. Lymperopoulou G, Pantelis E, Papagiannis P, Rozaki-Mavrouli H, Sakelliou L (2004) A Monte Carlo dosimetry study of vaginal ^{192}Ir brachytherapy applications with a shielded cylindrical applicator set. *Med Phys*, **31**: 3080-3086.
11. Mowlavi AA, Cupardo F, Severgnini M (2008) Monte Carlo and experimental relative dose determination for an Iridium-192 source in water phantom. *Iran J Radiat Res*, **6**: 37-42.
12. Andreo P (1991) Monte Carlo techniques in medical radiation physics. *Phys Med Biol*, **36**: 861-920.
13. Briesmeister JF (1997) MCNP-A general Monte Carlo N-particle transport code, Version 4B. Los Alamos National Laboratory Report. LA-12625-M.
14. Perez-Calatayud J, Ballester F, Serrano-Andres MA, Puchades V, Lluch JL, Limami Y, Casal F (2001) Dosimetry characteristics of the Plus and 12i GammaMed PDR ^{192}Ir sources. *Med Phys*, **28**: 2576-2585.
15. Ballester F, Puchades V, Lluch JL, Serrano-Andres MA, Limami M, Pérez-Calatayud J, Casal E (2001) Technical note: Monte-Carlo dosimetry of the HDR 12i and Plus ^{192}Ir sources. *Med Phys*, **28**: 2586-2591.
16. Shirley VS (1991) Nuclear data sheets for A=192. *Nuclear Data Sheets*, **64**:205-322.
17. Taylor REP and Rogers DWO (2008) EGSnrc Monte Carlo calculated dosimetry parameters for ^{192}Ir and ^{169}Yb brachytherapy sources. *Med Phys*, **35**: 4933-4944.
18. Lopez JFA, Donaire JT, Alcalde RG (2011) Monte Carlo dosimetry of the most commonly used ^{192}Ir high dose rate brachytherapy sources. *Rev Fis Med*, **12**: 159-168.
19. Naseri A and Mesbahi A (2009) Application of Monte Carlo calculations for validation of a treatment planning system in high dose rate brachytherapy. *Rep Pract Oncol Radiother*, **14**: 200-204.
20. Wallace S, Wong T, Fernando W (1998) Monte Carlo dosimetry of the microselectron HDR ^{192}Ir brachytherapy source using MCNP4A. *Australas Phys Eng Sci Med*, **21**:11-17.

